THE ASTROPHYSICAL JOURNAL, 261:595–611, 1982 October 15

THE CHEMICAL COMPOSITION OF R CORONAE BOREALIS AND XX CAMELOPARDALIS

P. L. COTTRELL AND DAVID L. LAMBERT
McDonald Observatory and Department of Astronomy, University of Texas at Austin
Received 1982 February 25; accepted 1982 April 26

ABSTRACT

Three R Coronae Borealis stars (R CrB, XX Cam, and RY Sgr) have been examined using extensive, high resolution, high signal-to-noise Reticon data. From He- and C-rich models and an appropriate model atmosphere code, the following atmospheric parameters were derived:

$$T_{\rm eff} = 7000\ {\rm K}, \quad \log g = 0.5, \quad \bar{\xi}_t = 8\ {\rm km\ s^{-1}}, \quad {\rm C/He} \sim 0.004 \quad \text{for R CrB},$$

$$T_{\rm eff} = 7000\ {\rm K}, \quad \log g \sim 0.0, \quad \bar{\xi}_t = 8\ {\rm km\ s^{-1}}, \quad {\rm C/He} \sim 0.003 \quad \text{for XX Cam}.$$

Insufficient data and a previously unreported spectral line-splitting prevented a detailed analysis of RY Sgr.

Elemental abundances were derived for a wide range of species. Pertinent ratios for R CrB and XX Cam are respectively -5.9 and < -8.6 for [H/He], $+2.7$ and $< +1.4$ for [Li/Fe], $+1.5$ and $+1.2$ for [C/Fe], $+1.1$ and $+1.4$ for [N/Fe], and $+0.9$ and $+0.8$ for [O/Fe]. Other elements (including both the light and heavy *s*-process) have approximately their solar abundance ratios.

The evolutionary history of these stars is discussed. We conclude that both CNO cycle and 3α processed material must have been mixed into the observable layers. We suggest the He core and He shell flashes as possible triggers for both this mixing and the extensive mass loss required to expose the heavily processed layers.

Subject headings: nucleosynthesis — stars: abundances — stars: individual (R CrB, XX Cam) — stars: mass loss — stars: R Coronae Borealis

I. INTRODUCTION

The R Coronae Borealis stars pose a rich array of fascinating and difficult questions for the stellar spectroscopist. These questions may be sorted into two nonorthogonal categories: "atmospheric structure" and "chemical composition."

At maximum light, the normal state for an R CrB star, many stars experience small amplitude ($\Delta m \lesssim 0.5$) pulsations with periods of ~ 40 to 120 days. A theoretical model of the pulsations is emerging (Cox *et al.* 1980). By contrast, the abrupt decline to minimum light at irregular intervals is not understood (e.g., see Feast 1975).

The composition is presumed to betray clues to the history and current behavior of these stars. The remarkable weakness of the hydrogen Balmer lines indicates a severe deficiency of hydrogen. The strongly enhanced neutral carbon lines hint at a C overabundance. In this paper, we report our new spectroscopic analysis. Our immediate goal was a determination of the abundances of the key light elements C, N, and O (also Li) because these may indicate the relative roles of the 3α process and the CNO cycles in defining the present atmospheric composition and, hence, the origin of these peculiar stars.

Three R CrB variables are discussed here: R CrB, XX Cam, and RY Sgr. Previous abundance analyses have been based largely upon relatively strong lines in the crowded blue to visible ($\lambda \lesssim 5000$ Å) interval. Continuum placement and line blending impair the measurement of equivalent widths. The strong lines are critically dependent on the microturbulent velocities and only moderately sensitive to the abundance. Published analyses include: Searle (1961) for R CrB; Danziger (1965) for RY Sgr; Orlov and Rodriguez (1974) for XX Cam; and Schönberner (1975) using the previously published data for all three of these stars. Our model atmosphere analysis is based on Reticon data in yellow and red spectral regions.

II. OBSERVATIONS

Extensive Reticon spectra of R CrB and XX Cam were obtained with the coudé spectrograph on the 2.7 m McDonald Observatory telescope (Vogt, Tull, and Kelton 1978). These observations encompassed key fea-

TABLE 1

WAVELENGTH REGIONS (λ_c)

	λ (Å)											
STAR	4840	5420	5550	5850	5960	6150	6370	6460	6550	6640	6730	9850
R CrB	√	√	√	√	√	√	√	√	√	√	√	√
XX Cam ...	√	√	√	√	√	√	√	√	√	√	√	√
RY Sgr.....	...	...	...	√	...	...	√	√	√	...	√	...

tures (e.g., the Balmer series lines, permitted and forbidden lines of carbon, nitrogen, and oxygen) from 4100 Å to ~1 μm. Selected wavelength regions were acquired for RY Sgr. Table 1 lists the central wavelengths, λ_c, of the spectra. Each spectrum covered ~100 Å. A resolution of ~0.3 Å was used for most observations, but the line widths are generally determined by the intrinsically large turbulent motions within the atmospheres of these supergiants (Schönberner 1975). All spectra were obtained during maximum light. R CrB was observed from March 1978 to August 1981. No significant changes in the spectrum were noticed over this period.

Equivalent widths (W_λ) measured from the above spectra are given in Table 2. Note that we are able to measure significantly weaker lines than any of the previous analyses of these stars. Our upper limits on the equivalent widths of absent lines are indicated by an "L" in Table 2.

Before proceeding with the detailed abundance analysis, we offer some spectral comparisons between the three R CrB stars. We adopt δ Canis Majoris (spectral type F8 Ia) as a comparison object of similar temperature and gravity and normal composition. Figures 1–4 illustrate the similarities and subtle differences between the three R CrB stars, and also the striking differences between these hydrogen-deficient stars and a normal supergiant. Figure 1 shows the extremely weak or absent Hα line. It is probable that XX Cam has no (detectable) hydrogen lines; Hβ is also absent. The line at 6562.1 Å in XX Cam has been identified by Hunger, Schönberner, and Steenbock (1982) as an absorption feature of neutral titanium. In R CrB and RY Sgr the apparent blueshifting of Hα is probably a result of blending of Hα with the Ti I line.

The region around the 6707 Å Li I resonance doublet is shown in Figure 2. Lithium was tentatively identified in R CrB by Keenan and Greenstein (1963). We confirm this identification. Our spectra also show that the Li I doublet is absent from XX Cam and RY Sgr. We suggest that earlier reports of Li in RY Sgr (Danziger 1965) and XX Cam (Rao, Ashok, and Kulkarni 1980) were probably in error. Hunger, Schönberner, and Steenbock (1982) also confirm the absence of the Li I line in XX Cam.

The C I lines have similar strengths in the three R CrB stars (Figs. 2 and 3). Indeed, neutral lines of all species ($Z > 8$) of both high and low first ionization potentials have a similar equivalent width in these R CrB variables. The metallic lines from the neutral atoms ($Z \geq 11$) are similar in the R CrB stars and δ CMa (Figs. 3 and 4). These latter figures also illustrate that He I, N I, and O I lines and ionized metallic lines are significantly stronger in XX Cam than in R CrB. For a comparison of the equivalent widths of lines of various elements we refer the reader to Table 2.

Our analysis of RY Sgr was abandoned when striking variations of the line spectrum were discovered (see, for example, Fig. 2). The absorption lines vary in strength and profile. At certain phases, the lines are split into two components with a separation of about 40 km s^{-1}. On some spectra, very weak emission lines (especially of Ti II) are seen. These variations possibly reflect changes in the atmospheric structure correlated with the $38^d.6$ pulsation period (Alexander *et al.* 1972). If these remarkable variations have existed throughout the lifetime of RY Sgr, it is puzzling that they went unnoticed by Danziger (1965) in his abundance analysis of this star. We should stress that R CrB and XX Cam, for which our observations are more extensive than for RY Sgr, show no hint of spectrum variations like those seen in RY Sgr.

III. THE ABUNDANCE ANALYSIS METHOD

a) *The* C/He *Ratio*

The atmosphere of an R CrB star is severely H deficient (Bidelman 1953). A plausible assumption is that the atmosphere is now dominated by nuclear processed material in which the initial H was converted to He. The presence of an extraordinary number of C I lines in the spectra would seem to imply that some of the synthesized He may have been burnt to C and, perhaps, O and other light α-rich elements. Since there is no *a priori* argument by which to determine the C/He ratio, a spectroscopic derivation is necessary.

The strength of an absorption line is controlled largely by the ratio of the line (κ_l) to continuous (κ_c) opacity.

TABLE 2

LINE AND EQUIVALENT WIDTH DATA

λ (Å)	MULTIPLET	EP (eV)	LOG *gf*	EQUIVALENT WIDTHS (mÅ) R CrB	XX Cam	RY Sgr
H I:						
4861.34 ...	1	10.20	−0.02	395	30L	
6562.81 ...	1	10.20	0.71	536	30L	477
He I:						
5875.63 ...	11	20.87	0.74	127	265	340
Li I:						
6707.85 ...	1	0.00	0.41	219	15L	15L
C I:						
4784.72 ...	18.04	7.95	−2.65	46	...	
4812.92 ...	5	7.48	...	299	305	
4817.37 ...	5	7.48	−2.68	330	306	
4826.80 ...	5	7.49	−2.33	326	283	
4836.76 ...	22.20	8.54	...	292	300	
4858.88 ...	22.19	8.54	...	275	264	
5912.58 ...	71	9.00	...	194	177	
5940.10 ...	26.12	8.64	−2.36	109	102	
5943.39 ...	70	9.00	−1.45	187	208	
5947.61 ...	26.12	8.64	...	127	124	
5950.04 ...	21.11	8.64	−2.13	122	92	
5957.56 ...	26.11	8.64	−2.08	246	278	
5963.99 ...	26.12	8.64	...	226	215	
5969.33 ...	17.20	7.95	...	238	239	
5970.73 ...	17.20	7.95	−2.91	116	74	
5972.59 ...	26.10	8.64	...	100	109	
5976.68 ...	26.09	8.64	...	135	150	
5981.22 ...	17.20	7.95	−3.03	160	117	
5996.06 ...	26.08	8.64	...	130	153	
6001.13 ...	26.07	8.64	−2.09	356	353	
6002.98 ...	26.08	8.65	...	287	309	
6006.03 ...	26.08	8.65	...	383	378	
6007.18 ...	26.07	8.64	...	298	331	
6010.68 ...	26.07	8.64	...	339	...	
6108.53 ...	36	8.85	...	231	212	
6115.85 ...	36	8.85	...	321	375	
6120.82 ...	36	8.85	...	327	255	
6413.55 ...	29.04	8.77	−1.85	...	298	242
6568.71 ...	61	9.00	...	298	353	296
6578.77 ...	60	9.00	−2.22	211	308	164
6586.27 ...	59	9.00	...	320	413	463
6587.62 ...	22	8.53	−1.30	524	485	450
6591.45 ...	35	8.85	−2.41	198	198	
6595.24 ...	35	8.85	−1.94	181	154	
6596.85 ...	35	8.85	...	240	288	
6659.31 ...	34	8.85	...	...	34	
6660.38 ...	34	8.85	−2.93	...	91	
6665.88 ...	34	8.85	−2.05	...	88	
6671.84 ...	33	8.85	...	...	300	
6674.11 ...	33	8.85	−2.01	...	372	
6683.95 ...	33	8.85	−2.03	225	239	
6688.79 ...	33	8.85	−1.98	249	240	
6711.29 ...	21.01	8.54	...	181	174	
9850.26 ...	1F	0.01	−10.80	108	60L	
C II:						
6578.05 ...	2	14.45	0.08	148	190	
6582.88 ...	2	14.45	−0.22	134	191	

TABLE 2—*Continued*

λ (Å)	Multiplet	EP(eV)	log *gf*	Equivalent Widths (mÅ) R CrB	XX Cam	RY Sgr
N I:						
6423.03 ...	21.03	11.76	−2.22	...	77	33
6436.71 ...	21.01	11.76	−1.39	...	50	45
6437.68 ...	21.02	11.75	−4.69	...	69	100
6440.94 ...	21.03	11.76	−1.14	75	167	110
6441.71 ...	21.03	11.76	−2.37	...	123	47
6457.90 ...	21.01	11.76	−2.17	123	185	
6468.44 ...	21.01	11.76	−3.74	...	152	
6483.75 ...	21	11.75	−1.04	169	298	
6484.80 ...	21	11.76	−0.76	145	256	
6506.31 ...	21	11.76	−3.37	...	207	165
6622.54 ...	20	11.76	−1.53	51	114	
6646.50 ...	20	11.75	−1.66	45	84	
6656.51 ...	20	11.75	−1.66	66	117	
6700.50 ...	59	11.84	−2.34	...	52	
6704.84 ...	59	11.84	−1.35	50	93	
6706.11 ...	59	11.84	−1.80	...	146	
6708.76 ...	59	11.84	−1.79	56	132	
6713.11 ...	59	11.84	−2.81	48	108	
6720.97 ...	58	11.84	−2.65	47	101	
6722.62 ...	59	11.84	−0.98	122	229	
6733.32 ...	58	11.84	−1.79	74	146	
6752.03 ...	58	11.84	−1.33	...	114	
9798.56 ...	19	11.75	−0.64	122	227	
9810.00 ...	19	11.75	−0.82	122	236	
9814.00 ...	19	11.76	−1.57	96	183	
9822.75 ...	19	11.76	−0.25	205	360	
9834.62 ...	19	11.76	−0.61	173	294	
9863.33 ...	19	11.76	0.00	229	405	
9872.15 ...	19	11.76	−0.65	166	273	
O I:						
5958.48 ...	23	10.99	−0.87	234	257	
6155.98 ...	10	10.74	−0.70	326	423	
6156.77 ...	10	10.74	−0.48	332	416	
6158.18 ...	10	10.74	−0.33	412	525	
6363.79 ...	1F	0.02	−10.25	93	82	75
6453.60 ...	9	10.74	−1.35	182	285	106
6454.45 ...	9	10.74	−1.13	226	252	
Na I:						
6154.23 ...	5	2.10	−1.51	113	153	
6160.75 ...	5	2.10	−1.20	210	312	
Al I:						
6696.03 ...	5	3.14	−1.57	86	80	
6698.67 ...	5	3.14	−1.90	63	68	
Si I:						
5948.55 ...	16	5.08	−1.30	257	209	
6125.03 ...	30	5.61	−1.78	124	204	
6131.72 ...	30	5.61	−1.47	133	...	
6145.02 ...	29	5.61	−1.51	96	128	
6555.47 ...	62	5.98	−1.15	206	190	
6719.62 ...	...	6.00	−1.83	70	96	
6721.84 ...	38	5.86	−1.25	112	105	
Si II:						
5978.91 ...	4	10.07	0.22	227	317	
S I						
6536.36 ...	...	8.05	−1.19	73	118	96
6743.58 ...	8	7.86	−0.62	178	184	
6748.78 ...	8	7.87	−0.48	227	214	
6757.20 ...	8	7.87	−0.22	241	...	

TABLE 2—*Continued*

λ (Å)	Multiplet	EP(eV)	log *gf*	Equivalent Widths (mÅ) R CrB	XX Cam	RY Sgr
Ca I:						
6122.23 ...	3	1.89	−0.26	378	373	
6162.18 ...	3	1.90	−0.04	325	300	
6166.44 ...	20	2.52	−1.12	68	51	
6439.08 ...	18	2.52	0.02	296	246	297
6449.82 ...	19	2.52	−0.64	217	161	209
6471.67 ...	18	2.52	−0.79	181	138	164
6493.79 ...	18	2.52	−0.29	329	277	254
Ca II:						
9854.67 ...	12	7.47	...	380	454	
Ti II:						
4865.62 ...	29	1.12	−2.84	360	321	
4874.01 ...	114	3.09	−1.00	379	350	
6559.57 ...	91	2.05	−2.51	263	316	308
V II:						
5928.89 ...	98	2.52	−1.62	154	212	
Cr I:						
4846.33 ...	208	3.45	...	62	80	
Cr II:						
4812.35 ...	30	3.86	−1.83	299	341	
4848.25 ...	30	3.86	−1.30	417	424	
4864.32 ...	30	3.86	−1.32	421	388	
4876.44 ...	30	3.85	−1.44	418	448	
Fe I:						
4787.83 ...	384	3.00	−2.55	27	19	
4788.77 ...	588	3.24	−1.77	44	51	
4789.66 ...	753	3.55	−1.14	142	160	
4872.14 ...	318	2.88	−0.56	352	291	
5916.26 ...	170	2.45	−2.86	90	100	
5930.19 ...	1180	4.65	−0.24	179	255	
5934.67 ...	982	3.93	−1.08	99	91	
6008.57 ...	982	3.88	...	171	205	
6136.62 ...	169	2.45	−1.42	272	294	
6137.70 ...	207	2.59	−1.39	246	282	
6170.52 ...	1260	4.79	−0.26	101	121	
6173.34 ...	62	2.22	−2.83	116	180	
6188.00 ...	959	3.94	−1.62	43	72	
6191.57 ...	169	2.43	−1.48	288	264	
6200.32 ...	207	2.61	−2.34	72	60	
6419.96 ...	1258	4.71	−0.30	185	202	224
6421.36 ...	111	2.28	−2.00	215	195	291
6430.86 ...	62	2.18	−2.00	214	182	265
6469.19 ...	1258	4.83	−0.66	71	64	134
6475.63 ...	206	2.56	−2.79	73	51	133
6494.99 ...	168	2.40	...	355	328	332
6546.25 ...	268	2.76	−1.66	154	222	185
6592.93 ...	268	2.73	−1.54	203	234	145
6593.88 ...	168	2.43	−2.27	104	108	184
6750.16 ...	111	2.42	−2.55	84	76	
9861.79 ...	1296	5.04	...	75	119	
Fe II:						
4833.19 ...	30	2.66	−4.61	211	275	
4840.00 ...	30	2.68	−4.66	281	287	
4868.81 ...	30	2.68	...	56	118	
5991.38 ...	46	3.15	−3.63	316	405	
6149.25 ...	74	3.89	−2.77	368	486	
6175.16 ...	200	6.22	−2.20	236	339	
6179.40 ...	163	5.57	−2.57	169	283	
6416.93 ...	74	3.89	−2.73	330	466	377
6432.68 ...	40	2.89	−3.64	304	423	410
6442.95 ...	...	5.55	−2.52	132	208	166
6446.40 ...	199	6.22	−1.98	119	252	141
6493.06 ...	...	5.58	−2.48	237	339	279
6516.08 ...	40	2.89	−3.38	356	527	

TABLE 2—*Continued*

λ (Å)	Multiplet	EP(eV)	log *gf*	Equivalent Widths (mÅ) R CrB	XX Cam	RY Sgr
Co I:						
4867.87 ...	...	3.12	0.38	124	69	
Ni I:						
4786.54 ...	98	3.42	−0.19	244	...	
4829.03 ...	131	3.54	−0.35	155	171	
4831.18 ...	111	3.61	−0.46	151	191	
4857.40 ...	111	3.74	−0.82	103	94	
4866.28 ...	111	3.54	−0.52	234	198	
6767.78 ...	57	1.83	−2.08	119	...	
6772.32 ...	127	3.66	−0.98	64	...	
Ni II:						
6195.36 ...	...	14.50	...	...	220	
6433.77 ...	...	15.00	...	143	184	186
6459.74 ...	...	14.70	...	...	61	53
6487.23 ...	...	15.00	...	57	128	80
6541.19 ...	...	15.00	...	56	89	69
Y II:						
4883.69 ...	22	1.08	−0.05	446	517	
5402.78 ...	35	1.84	−0.43	162	204	
5521.59 ...	27	1.74	−0.91	123	103	
Ba II:						
5853.68 ...	2	0.60	−1.27	459	358	
6141.73 ...	2	0.70	−0.07	432	538	
6496.91 ...	2	0.60	−0.43	508	530	641
Nd II:						
4811.35 ...	3	0.06	−0.42	63	62	
5431.53 ...	80	1.12	0.05	107	94	
5842.39 ...	86	1.28	−0.23	78	141	

In normal stars, κ_c is generally dominated by contributions dependent on the H density, and therefore the abundance[1] X/H is obtained quite naturally from analysis of lines attributable to element X. Earlier work (see particularly Schönberner 1975) shows that C is the leading contributor to κ_c (unless the C/He ratio is extremely small) and hence the abundance ratio X/C is readily obtainable from the spectrum. Since C is most probably a minor species (C/He $\ll 1$), not only do we need the C/He ratio in our search for the origin of the R CrB stars but this ratio also influences the atmospheric structure which we must know before we can analyze the spectrum. In this section, we sketch arguments previously employed by Schönberner (1975) to set upper and lower limits on the C/He ratio. We also note that the ratio is directly obtainable from measurements of He I lines (Fig. 3).

The assumption that the mass fraction of heavy elements ($Z \gtrsim 16$) has not been changed by nuclear burning is employed to set an upper limit on the C/He ratio. Line analysis gives the ratio $r_X(\text{R CrB}) = f_X/f_C$, where f denotes a mass fraction and X is an element heavier than sulfur. Since the R CrB stars do not belong to the extreme Population I, we may suppose that their initial metal content did not exceed the solar value. Then

$$f_X(\text{R CrB}) = r_X(\text{R CrB}) f_C(\text{R CrB}) \leq f_X(\odot),$$

or

$$f_C \leq f_X(\odot)/r_X(\text{R CrB}).$$

Detailed analysis (see § IV*a*) gives C/He ≤ 0.03 (R CrB) and ≤ 0.01 (XX Cam), where $f_{He} + f_C + f_N + f_O \approx 1$. Our limit is a factor of 3 less than the limit set by Schönberner by the same arguments. This difference in part reflects the lower continuous opacity employed by us (see § III*b*). However, the major factor is our use of much weaker lines, which are less dependent upon the microturbulence.

A lower limit to C/He is provided by the observed equivalent widths of C I lines of known oscillator strength. If C/He exceeds some minimum value, then C is the dominant contributor to κ_c and the equivalent width of a C I or C II line is then effectively independent of C/He. The equivalent width is, of course, affected by the effective temperature, the surface gravity, and microturbulence. (The C/He ratio will affect the atmospheric

[1]Where this denotes the ratio of these species by number.

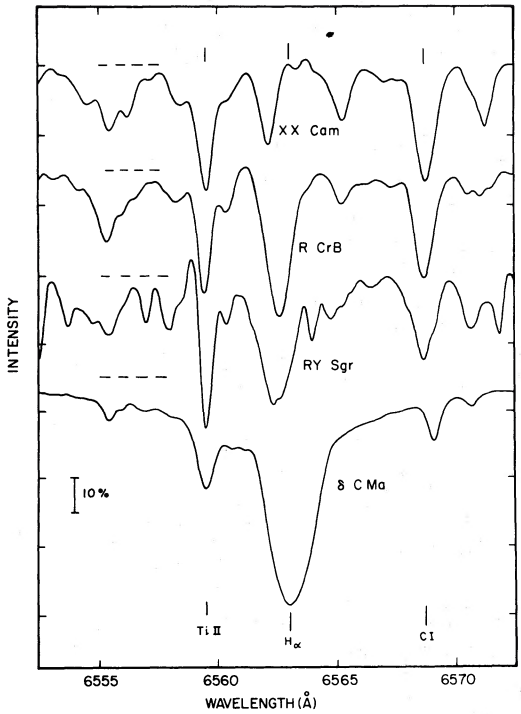

FIG. 1

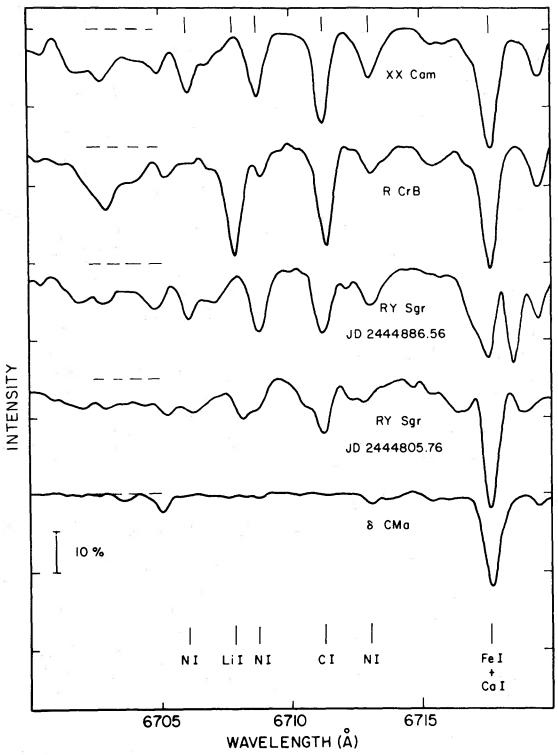

FIG. 2

FIG. 1.—Spectra of the three R CrB stars in the region of Hα. The star δ CMa (a normal composition F8 supergiant) is included as a comparison object. Our continuum placement is indicated by the dashed line and the positions of the important features are shown.

FIG. 2.—The interval around Li I at 6707 Å; see legend to Fig. 1

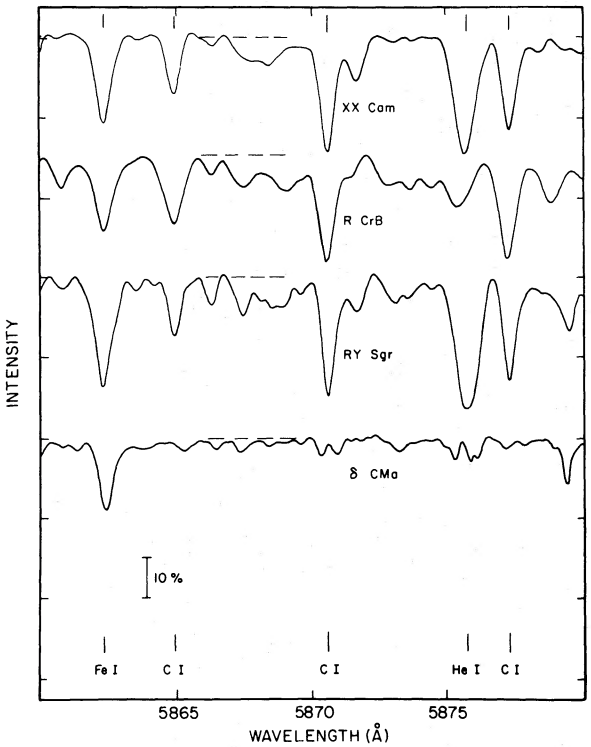

FIG. 3.—The interval near the He I line at 5876 Å; see legend to Fig. 1.

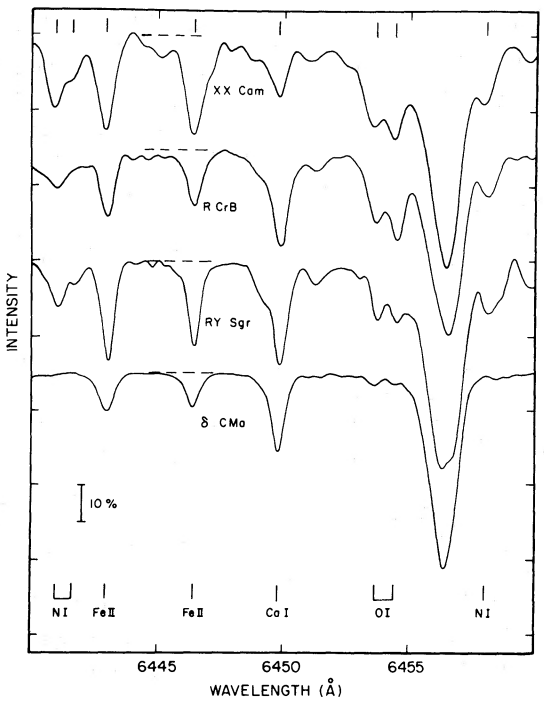

FIG. 4.—Selected N I and O I lines near 6450 Å; see legend to Fig. 1.

structure and so indirectly influence the equivalent widths.) If C/He is too small, the contribution of C to κ_c is negligible and the equivalent width of a C line is dependent on the C/He ratio. Schönberner set C/He $\geq$ 0.01 in R CrB, XX Cam, and RY Sgr from observations of strong C I lines. With access to weak C I lines, we obtain lower limits: C/He $\gtrsim$ 0.003 (R CrB) and 0.002 (XX Cam). These lines are almost independent of the adopted microturbulent velocity and the atmospheric parameters.

Keenan and Greenstein (1963) reported the presence of the He I line 5876 Å in the spectrum of R CrB. We confirm this identification and show that the line is considerably stronger in XX Cam and RY Sgr (see Fig. 3). If this is a photospheric line which is formed in LTE, it gives a direct estimate of the C/He ratio. This abundance would seem to be very dependent on the adopted effective temperature, but this dependence is reduced considerably by analyzing the He I lines relative to the C II lines. Unfortunately, the chromosphere may contribute to the 5876 Å triplet. Querci and Querci (1978) reported the He I 10830 Å line to have a P Cygni profile in a spectrum of R CrB taken 1 mag below maximum light. They attributed the line to the circumstellar shell. In contrast, Zirin (1982) reports the He I 10830 Å line to be absent ($W_\lambda \lesssim 70$ mÅ) in his higher dispersion spectra taken in 1978 July when R CrB was at maximum light. The fact that Zirin's upper limit for the W_λ (10830 Å) is inconsistent with the Querci and Querci (1978) measurement and our W_λ (5876 Å) may indicate a variable chromospheric structure. The chromospheric (i.e., NLTE) contribution should be greatly reduced for the singlet He I lines. Unfortunately, the 6678 Å line, which is the most promising candidate for detection, is severely blended. The rough estimate of its equivalent width is just consistent with the above lower limits: C/He $\sim$ 0.004 (R CrB) and 0.003 (XX Cam). In view of our inability to test fully for a chromospheric contribution, we do not further pursue this direct approach to the C/He ratio.

b) Model Atmospheres and the Line Analysis Program

All the models used in the present analysis were supplied by Dr. D. Schönberner (see Schönberner 1975). We used models with effective temperatures ($T_{\rm eff}$) of 6000 K and 7000 K, gravities (log g) of 0.0 and 0.5, and a variety of abundances. The helium abundances range from 90 to 99% by number, with carbon accounting for the remainder.[2] All other elements have their solar mass fractions. The flux-constant models were constructed with the usual assumptions of plane-parallel geometry, hydrostatic and local thermodynamic equilibrium.

[2]Model atmospheres are indicated thus; He:C = 90:10 implies 90% He and 10% C by number.

To analyze the equivalent widths, we utilized the line analysis program WIDTH, which was written by Dr. R. L. Kurucz. This particular code is well suited to the present problem in which hydrogen is not the dominant species. Specifically, WIDTH and its parent program ATLAS (see Kurucz 1970) are structured such that the abundances are determined relative to the total number of atoms [in normal stars this is effectively (H + He)]. In the current work, the composition of the atmosphere is predominantly He + C (Schönberner 1975).

The unusual composition led us to consider which opacities are dominant and whether they have been represented realistically in the codes. As was suggested by Searle (1961) and confirmed by Schönberner (1975), neutral carbon (both bound-free and free-free processes) is the dominant opacity source in these H-deficient, He- and C-rich atmospheres. For models with $T_{\rm eff} \sim 7000$ K, carbon is also the principal source of electrons for the second most important opacity, He^-. Thus, carbon determines the transparency of the atmosphere while helium is the dominant contributor to the mean molecular weight and, therefore, the gas pressure.

In WIDTH (and also ATLAS), C I bound-free and free-free opacity are only considered for $\lambda < 1445$ Å. For the H-deficient carbon stars, bound-free transitions from many more levels of neutral carbon and also the C I free-free opacity must be considered. Peach (1970) provides absorption cross sections (both bound-free and free-free) for several neutral and ionized elements (including C I) up to wavelengths of 7100 Å. She also provides equations and tables for calculating the free-free opacity to longer wavelengths. Tables from Travis and Matsushima (1968) were used to extend the C I bound-free absorption cross sections to $\lambda > 7100$ Å. In the region of overlap—5000 and 7100 Å—there is excellent agreement between Peach (1970) and Travis and Matsushima (1968).

Apart from photoionization of neutral carbon and the He^- opacity, the next most important continuous opacity source is C^- (which was *not* included in the original version of WIDTH). C^-, while it is important at the cooler end of the temperature range, is a minor contributor to the total opacity (even at $T_{\rm eff} = 6000$ K). We included C^- in our version of WIDTH by coding the opacity tables of Myerscough and McDowell (1966).

From a preliminary abundance analysis, we deduced that all other standard opacity sources (e.g., H I and H^- bound-free and free-free processes) were insignificant relative to those discussed above. Both N I and O I could probably provide additional continuous opacity. However, we find that oxygen and nitrogen in R CrB are about one-third as abundant as carbon. Then, the total contribution of N and O to the opacity is not more than about 3% for the hotter models.

The output accompanying the models used in this analysis (Schönberner, private communication to

D. L. L.) also included the total opacity as a function of optical depth and wavelength. Comparison of these values with those calculated using WIDTH (with the modifications discussed above) showed that the former were larger by ~ 0.2 dex. A number of effects could contribute to this discrepancy. First, we have no detailed information about individual opacity sources used by Schönberner and, thus, we cannot isolate a specific opacity as the source of the difference. Second, we considered only C I, C^-, and He^- and electron scattering as contributing to the total opacity in the WIDTH analysis. Small contributions ($\sim$1–5%) from several other sources (N I, O I, and the metals) would increase the total opacity computed by WIDTH. This discrepancy in the computed total opacity suggests that we use some caution in the interpretation of an absolute abundance scale. The discrepancy should have a much smaller influence on abundance ratios.

c) *Oscillator Strengths*

The oscillator strengths (see Table 2) used in this analysis were gleaned from a variety of sources. For H I, He I, Li I, and O I (permitted and forbidden) the *f*-values came from Wiese, Smith, and Glennon (1966). The oscillator strengths for N I came from the semiempirical calculations of Kurucz and Peytremann (1975). These determinations, at least for multiplet 19, agree well with the experimental values tabulated by Richter (1961). All other *gf*-values, except for those for carbon, were derived by analyzing the solar equivalent widths measured off the Liège Solar Atlas (Delbouille, Roland, and Neven 1973) with the Holweger-Müller (1974) solar model, the Ross and Aller (1976) solar abundances and a line analysis model atmosphere program (LINES: Sneden 1974). A few C I *gf*-values were derived from solar lines, but most of the lines in which we were interested were too weak. Unfortunately, adequate theoretical calculations of the *gf*-values for a majority of the C I transitions are not yet available; severe cancellation affects many of the radial integrals (Lambert 1968), and configuration interaction is an additional complexity.

d) *Atmospheric Parameters*

We use standard techniques to obtain the atmospheric parameters: $T_{\rm eff}$, $\log g$, and ξ_t. First, $T_{\rm eff}$ is set by the requirement that the abundance of a species be independent of the lower excitation potential (χ) of the line. Second, the surface gravity is provided by the condition that neutral and ionized lines of an element give the same abundance. Third, the requirement that individual abundances from lines of a single species be independent of the reduced width ($\log W_\lambda/\lambda$) provides the microturbulent velocity.

i) $T_{\rm eff}$

Initially, we planned to combine the numerous permitted C I lines with one or more of the [C I] lines. The large range of lower excitation potential ($\Delta\chi \sim 9$ eV) would have yielded a precise temperature. However, two difficulties—the lack of reliable *gf*-values for many of the permitted transitions and the large change in continuous opacity across the wavelength baseline ($\chi = 0$ eV at 9850 Å, $\chi = 9$ eV lines between 6000 and 7000 Å)—forced us to discard C I. (Note the [C I] 8727 Å line is badly blended.) Oxygen provides the forbidden ($\chi = 0$ eV) line at 6363.8 Å as well as the permitted lines at 6150 Å (multiplet 10) and 6450 Å (multiplet 9). The other [O I] lines at 5577 Å and 6300 Å are blended. These transitions fall within a narrow wavelength range and provide a larger χ baseline ($\Delta\chi = 11$ eV) than the C I lines ($\Delta\chi = 9$ eV). Neutral and ionized lines of iron with $\Delta\chi = 2.9$ and 2.6 eV are used as subsidiary temperature indicators.

Several investigators (Myerscough 1968; Rao, Ashok, and Kulkarni 1980; Fernie 1982) have utilized the energy distributions of R CrB stars to derive $T_{\rm eff}$. Our poor knowledge of the atmospheric structure, difficulties in estimating the amount of line blanketing and the unknown amounts of circumstellar material which will adjust the flux distribution in the infrared region make this a very imprecise method.

ii) $\log g$

In the observed wavelength intervals, only iron provides a sufficient number of neutral and ionized lines to give a reliable determination of the spectroscopic gravity. For nickel, the only other element for which there were several lines of two successive ionization states, imprecise empirical oscillator strengths for the ionized lines lead to large uncertainties in the inferred abundances.

iii) *The Microturbulence,* ξ_t

A few species (O, I, Fe I, Fe II) had sufficient range in reduced width for ξ_t to be derived. Several other species were shown to be consistent with the derived value, and an overall mean microturbulent velocity ($\bar{\xi}_t$) was obtained for each star.

IV. THE ABUNDANCE ANALYSIS: RESULTS

a) *Atmospheric Parameters*

Figures 5*a* and 5*b* show the individual abundances derived for R CrB from the oxygen lines, plotted against low excitation potential and reduced width, respectively, and for three values of microturbulence. These abundances were derived using a $T_{\rm eff} = 7000$ K, $\log g = 0.5$,

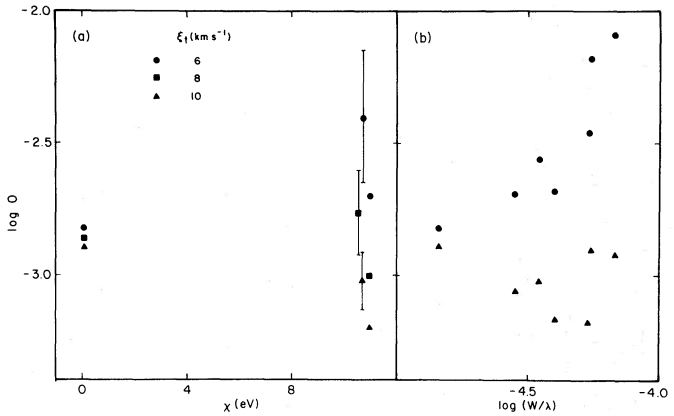

FIG. 5.—Derived oxygen abundances for R CrB as a function of (*a*) lower excitation potential (χ) and (*b*) reduced equivalent width (log W/λ). These abundances were determined using $T_{\rm eff} = 7000$ K, log $g = 0.5$, He:C = 99:1 model.

He:C = 99:1 model. These figures indicate that this model is consistent with the observational data and thus provides a good estimate for the effective temperature and the gravity for R CrB. Figure 6 also provides confirmation of our adopted $T_{\rm eff}$ (= 7000 K) because abundances from both Fe I and Fe II lines are independent of χ. From Figures 5*b* and 6*b*, ξ_t(O I) = 8.5 km s^{-1} and $\xi_t = 8$ km s^{-1} for neutral and singly ionized iron, respectively. All other species are consistent with a microturbulence of 8 km s^{-1}.

The C/He ratio is here classified as an atmospheric parameter. In § III*a* we noted that upper and lower limits can be set on the C/He ratio. The analysis of the He I lines and the determination of the limits were conducted using the basic atmospheric parameters ($T_{\rm eff}$, log g, and ξ_t) and the model atmosphere grid computed for He:C = 90:10, 97:3, and 99:1.

The 5876 Å He I line provides the C/He ratios: 0.004 (R CrB) and 0.003 (XX Cam), where we use the model grid to extrapolate to find the self-consistent C/He ratio of the model which returns the same ratio from the 5876 Å line. There is one other He I line which might be detectable: the equivalent width of 6678 Å in LTE at 7000 K is about one-half the 5876 Å equivalent width. Unfortunately, the 6678 Å He I line is severely blended; the limit $W_\lambda \lesssim 50$ mÅ is consistent with the 5876 Å measurements but, of course, does not test the possibility that the 5876 Å line is enhanced by chromospheric and/or NLTE contributions.

Our abundance analysis for R CrB and XX Cam was conducted using the model atmospheres computed for He:C = 99:1 and a solar mix of metals. Within the rather large uncertainties, this model provides a self-consistent C/He solution from the He I 5876 Å line just within the upper and lower bounds outlined in § III*a*. Abundances relative to C (or a metal such as Fe) for all elements except He should not be affected significantly by our use of the He:C = 99:1 model.

The adopted atmospheric parameters for R CrB and XX Cam are shown in Table 3.

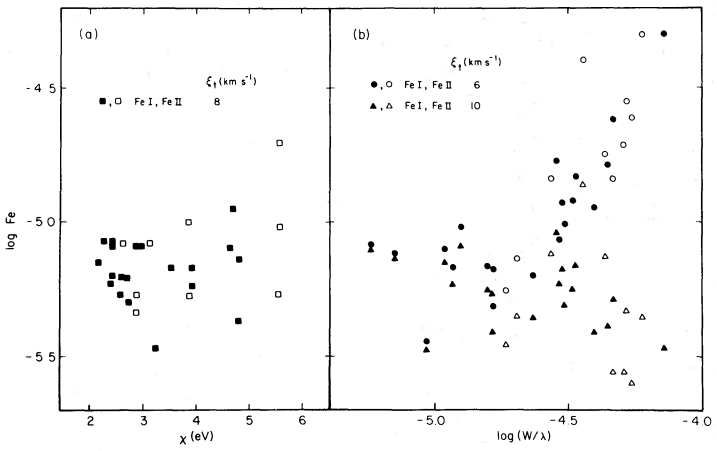

FIG. 6.—Derived iron abundances for R CrB for Fe I (*filled symbols*) and Fe II (*open symbols*) lines; see legend to Fig. 5

TABLE 3

ATMOSPHERIC PARAMETERS

Quantity[a]	R CrB	XX Cam
$T_{\rm eff}$ (K)	7000±250	7000±250
log g (cgs)	0.5±0.3	0.0±0.3
ξ_t (km s^{-1}) ...	8±1	8±1
C/He[b]	0.004 (0.003–0.03)	0.003 (0.002–0.01)

[a] The abundances He and C are number fractions relative to the total number of particles of all species.

[b] Derived using He I 5876 Å. Values in parentheses show the upper and lower limits derived in § III*a*.

b) *Individual Abundances*

Figures 7*a* and 7*b* (also Table 4) display our abundance results for R CrB and XX Cam, respectively. We discuss the individual abundances of R CrB and XX Cam in more detail. Brief references will be made to RY Sgr where appropriate.

i) [H/He] *Ratio*

This ratio varies between less than $10^{-8.5}$ (XX Cam) and $\sim 10^{-6}$ (R CrB and RY Sgr). The helium abundance is based solely on the D_3 line at 5876 Å (see § III*a*).

ii) Li

As we discussed in § II, we detect the Li I 6707 Å line only in R CrB (Fig. 3), the other two stars providing upper limits to the lithium abundance. R CrB has an almost cosmic abundance. This is approximately 15 times larger than the limits derived for XX Cam and RY Sgr.

iii) CNO

We derived these elemental abundances simultaneously with the helium abundance. The abundance ratios are C:N:O = 10:1:5 (R CrB), = 10:3:5 (XX Cam). In contrast, the solar ratio is 5:1:9 (Lambert 1978).

The carbon abundance (i.e., relative to the total number of atoms) has been discussed extensively in §§ III*a* and IV*a*. Nitrogen shows a large scatter among the abundances (i.e., relative to C) determined from lines of different multiplets. This may be due in part to the use of theoretical (intermediate coupling) oscillator strengths. Lines of multiplet 19 (near 9850 Å) for which experimental oscillator strengths have been determined (Richter 1961) have been adopted as our primary source of a N abundance. Lines of multiplet 20 (near 6650 Å) whose derived abundances are consistent (scatter $\lesssim 0.2$ dex) with multiplet 19 are used as a secondary indicator. The oxygen abundances are derived from well-studied multiplets (1F, 9, and 10). Although many of these lines are strong, the weak forbidden line at 6363 Å provides a reliable oxygen abundance.

Before completing the discussion of the CNO abundances, we comment on the $^{12}C/^{13}C$ ratio in the R CrB stars. This ratio is a trademark of the CNO nuclear burning cycles. For R CrB and XX Cam, we obtained spectra of the $\Delta v = -1$ bands of the Swan system of C_2 (Fig. 8). Although the (1,2) $^{12}C_2$ band head at 5585.5 Å is quite prominent in R CrB, there is no trace of the $^{12}C^{13}C$ lines which form a band head at 5577.0 Å. In fact, this region probably provides the best opportunity to derive a lower limit on the $^{12}C/^{13}C$ ratio. We estimate $^{12}C/^{13}C \gtrsim 40$, which is far removed from the equilibrium ratio of the CNO burning cycle ($^{12}C/^{13}C \approx 3.4$). For XX Cam, the $^{12}C^{12}C$ and $^{12}C^{13}C$ band heads are extremely weak or absent.

iv) Na *through* S

With the exception of Na, this group of elements in R CrB and XX Cam have abundances slightly in excess of solar values (Fig. 7 and Table 4). Sodium, which shows an overabundance relative to Fe and is more abundant in XX Cam than R CrB, is here represented by just two lines. Note that Ca, which should closely follow Na in its sensitivity to errors and changes in the atmospheric structure, is not overabundant.

v) Ca *through* Ni

The relative abundances of these elements (i.e., X/Fe) are close to the solar ratios in both R CrB and XX Cam. Although the effect is not large, there appears to be a real difference between this group of elements and the elements aluminum, silicon, and sulfur.

vi) *The s-Process Elements* (Y, Ba, Nd)

Within the observed wavelength intervals there are few unblended lines of these elements. On the basis of three strong Ba lines ($W_\lambda > 350$ mÅ), we derive a slight Ba overabundance. However, the large uncertainty implies that this is also consistent with a normal abundance. For the weaker lines of yttrium and neodymium, we derive solar abundances. Therefore, we conclude that the light (Y) and heavy (Ba, Nd) *s*-process elements have normal abundances relative to the total number of atoms.

vii) *Summary and Error Analysis*

With the exception of H, Li, N, and possibly Na, the derived abundances of all species are almost identical in R CrB and XX Cam. By inspection, we infer that the composition of RY Sgr must be generally similar. In addition, for elements heavier than sulfur ($Z = 16$), there is little difference between our relative abundances for these R CrB stars and the Sun. The enhancements of sodium and nitrogen in XX Cam relative to R CrB appear to be real abundance effects.

Rough error estimates were obtained from the Schönberner model atmosphere grid and the uncertain-

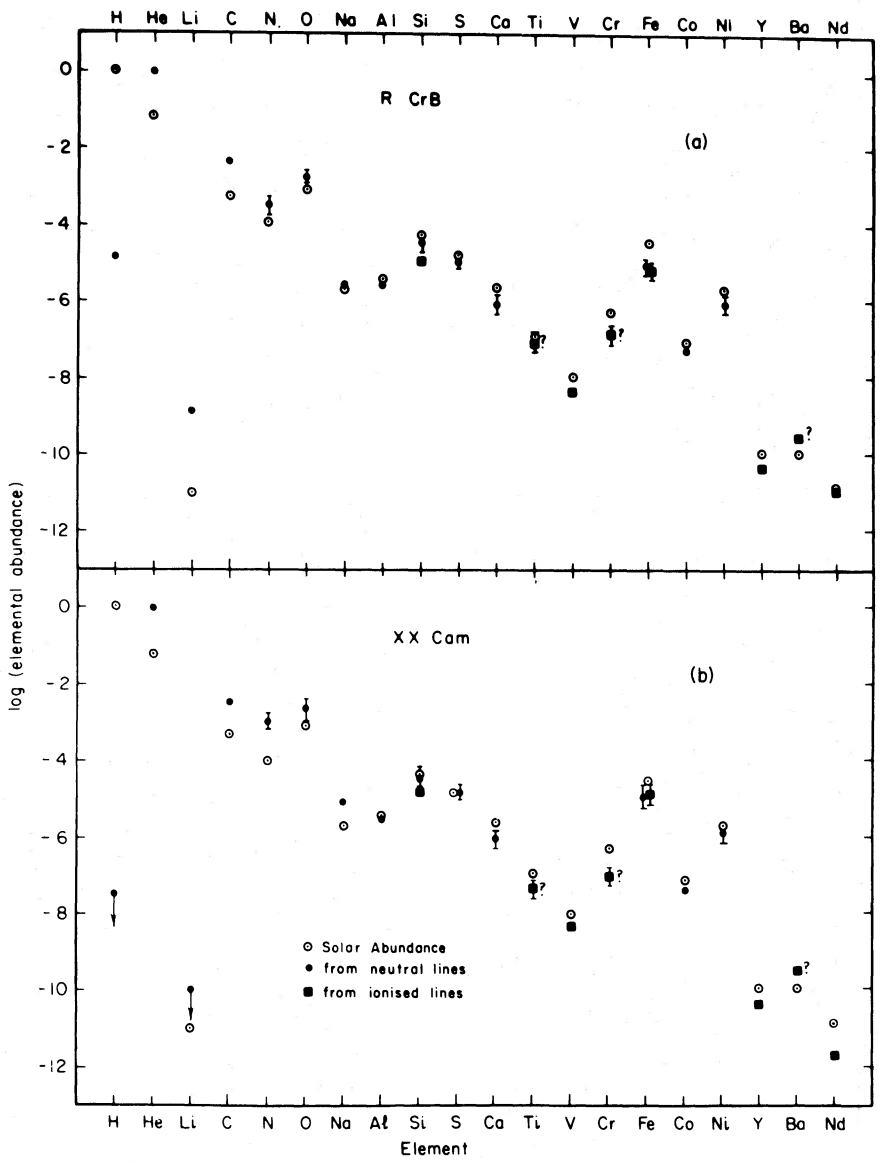

FIG. 7.—Elemental abundances for (*a*) R CrB and (*b*) XX Cam. The abundances are all logarithmic and relative to the number of atoms being set to 1 (0.0 dex). The solar abundances are from Ross and Aller (1976) except for CNO which are taken from Lambert (1978). The error bars included when abundances are derived from more than two lines and indicate the 1 σ spread around the mean abundance. The question marks indicate uncertain abundance determinations; i.e., those which utilized lines stronger than 250 mÅ (log $W_\lambda/\lambda \gtrsim -4.4$). The downward pointing arrows indicate upper limits.

ties in the atmospheric parameters (see Table 3). Elements were split into three groups—I, II, and III (see Table 5). The error estimates have been used in the compilation of Table 4. Such estimates do not, of course, include a contribution from failures of the underlying assumptions (departures from LTE and hydrostatic equilibrium, etc.).

A thorough theoretical exploration of the departures from LTE in the numerous species investigated here must await the availability of the necessary wide range of atomic data on radiative and collisional rates. An empirical study could be usefully undertaken from high-quality spectra over the widest possible wavelength interval and a detailed consideration of all lines of a given element. Our contention is that the non-LTE effects appear not to be a major source of error in this abundance analysis for the following reasons:

1. Elements from Na and up the periodic table display (LTE) abundances generally consistent with solar system values. With the possible exception of the *s*-process elements, these elements are indeed expected on sound theoretical grounds to preserve their initial (i.e.,

TABLE 4

INDIVIDUAL ABUNDANCES[a]

Ratio	R CrB	XX Cam
[H/He]	-5.9 ± 0.3	$<-8.6\pm0.3$
[Fe/total][b]	-1.1 ± 0.2	-0.8 ± 0.2
[Li/Fe]	$+2.7\pm0.3$	$<+1.4\pm0.3$
[C/Fe]	$+1.5\pm0.2$	$+1.2\pm0.2$
[N/Fe]	$+1.1\pm0.2$	$+1.4\pm0.2$
[O/Fe]	$+0.9\pm0.2$	$+0.8\pm0.2$
[Na/Fe]	$+0.7\pm0.2$	$+1.0\pm0.2$
[Al+Si+S/Fe]	$+0.4\pm0.1$	$+0.3\pm0.1$
[Ca+V+Co+Ni/Fe]	$+0.2\pm0.1$	$+0.1\pm0.1$
[Y+Nd/Fe]	$+0.3\pm0.2$	-0.2 ± 0.2

[a]Relative to solar abundances from Lambert 1978 for C, N, and O, and from Ross and Aller 1976 for all other elements.

[b]Note iron abundance is relative to the total mass, where $(\Sigma\mu_i n_i)=12.15$ (see Schönberner 1975).

TABLE 5

ABUNDANCE TRENDS[a]

Parameter	I[b]	II[c]	III[d]
$\Delta T=-1000$ K	-1.0	-0.5	$+0.3$
$\Delta \log g=-0.5$	$+0.3$	$-0.1\rightarrow+0.2$	-0.1
Δ[99/1 to 97/3]	$+0.5$	$+0.5$	$+0.5$
$\Delta\xi_t=+2$ km s^{-1}[e]	...	$-0.1\rightarrow-0.4$	...

[a]Expressed in dex and applies to all elements studied except He and C.

[b]Group I refers to neutral lines of low-to-moderate I.P. ($\lesssim$7.5 eV) elements (e.g., Na, Ca, Fe).

[c]Group II refers to neutral high excitation potential lines of moderate I.P. elements (e.g., Si, S) and abundances derived from all ionized lines (e.g., Ti, Cr).

[d]Group III is H, N, O.

[e]All groups affected similarly within the log W_λ/λ range -5.2 to -4.4.

solar system) relative abundancess as the R CrB star is produced. Our LTE analysis is consistent with this expectation. Note that the line sample includes both low and high excitation (e.g., S I) lines and neutral and ionized lines from several elements.

2. LTE analyses of O-rich supergiants of a similar $T_{\rm eff}$ also retrieve relative abundances in good agreement with solar system values (Luck and Lambert 1981; Luck 1982). Moreover, the CNO abundances obtained in these analyses are generally compatible with the theoretical predictions.

3. In our analysis, we strived to use weak lines whenever possible. Weak lines of high excitation potential (e.g., C I, N I, O I) are formed quite deep in the photosphere where non-LTE effects could be minimal. Our O abundance is based on the weak forbidden [O I] line which should not show severe departures from LTE.

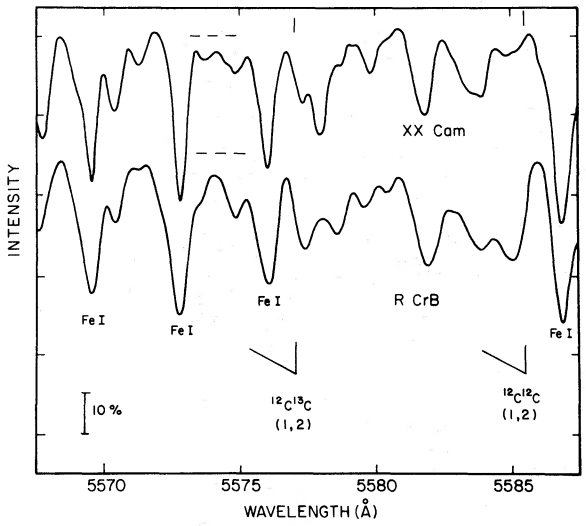

FIG. 8.—Spectra of R CrB and XX Cam in the vicinity of the $\Delta v=-1$ bands of C_2. The positions of the $^{12}C^{12}C$ (1,2) and $^{12}C^{13}C$ (1,2) band heads as well as some Fe I lines are shown.

V. PREVIOUS ABUNDANCE ANALYSES

Abundance analyses of R CrB stars have been reported by Searle (1961, R CrB), Danziger (1965, RY Sgr) and Orlov and Rodriguez (1974, XX Cam). Except for the *s*-process elements, we shall not compare our abundances with the results of these earlier analyses because, fortunately, Schönberner (1975) has reanalyzed the published equivalent widths of these three R CrB variables using model atmospheres. He considered only a small selection of the elements previously analyzed: H, He, C, O, Mg, Ti, and Fe. He adopted a C/He ratio of 0.03, and derived all abundances relative to this value. At this C/He ratio, our abundances are consistent with his for those elements in common (H, Ti, Fe).

Recently, Rao, Ashok, and Kulkarni (1981) and Hunger, Schönberner, and Steenbock (1982) discussed the Li abundance in R CrB stars. Rao *et al.* misidentified Li in XX Cam. As Hunger *et al.* note and our Figure 2 confirms, the 6707 Å Li I doublet is not present in XX Cam. Our spectra of RY Sgr also show that Li I is absent. Hence, we do not confirm Danziger's identification of Li in RY Sgr. The Li I doublet is certainly present in R CrB, as Keenan and Greenstein (1963) suggested.

Finally, we comment on the *s*-process elements. Schönberner (1975) did not include *s*-process elements in his reanalysis. Searle (1961), Danziger (1957), and Orlov and Rodriguez (1974) found that the *s*-process elements had normal abundances relative to iron. Hunger, Schönberger, and Steenbock (1982) observed the Ba II 6141 and 5854 Å lines in R CrB and XX Cam. Their model atmosphere analyses suggest a mean Ba

overabundance relative to Fe and Ca of about 1.0 dex. The Ba II lines are strong ($W_\lambda \gtrsim 350$ mÅ) so that the abundance uncertainties are large. Our independent analysis of the Ba/Fe ratio from the same Ba II lines also indicates a similar Ba overabundance. However, Y and Nd which provide much weaker lines ($W_\lambda \lesssim 100$ mÅ) are not overabundant according to our analysis. Therefore, we suggest that the *s*-process elements are not overabundant in either R CrB or XX Cam. Of course, we cannot exclude enrichment of these atmospheres with material having a nonstandard distribution of *s*-process abundances; for example, Bond, Luck, and Newman (1979) found that Sr and Y were approximately 100 times overabundant but Ba had a normal abundance in U Aqr, a cool R CrB star. This result can be readily understood in terms of *s*-processing by a single burst of neutrons. However, no simple variant of this scheme is likely to explain the apparent overabundance of Ba with the normal abundances of Y and Nd because Nd should closely follow Ba. Our preferred explanation is that the Ba abundance is in error because it is based on strong lines.

VI. THE NUCLEAR HISTORY OF R CORONAE BOREALIS VARIABLES

a) *The* CNO *Cycles and the 3α-Process*

The history of nuclear processing, mixing, and mass loss is recorded in the chemical composition of the R CrB atmosphere. We discuss this composition in terms of processing wrought by the CNO cycles and the 3α process. We omit the *s*-process because both R CrB and XX Cam have normal *s*-process abundances. Li production is attributed to the ^{7}Be-transport mechanism.

Qualitatively, our results for the R CrB stars are indicative of a He- and N-rich zone (in which essentially all the H has been processed through the CNO cycle), into which 3α processed material has been mixed. In the following discussion we concentrate on our novel results for He, C, N, and O. An additional constraint which must be folded into any production scenario for the R CrB variables is the paucity of these objects in the Galaxy. This indicates that the evolution through this phase must be extremely rapid and/or the type of structure described above is produced in only a small percentage of stars.

The remarkable H deficiency shows that the fraction of pristine material in the atmosphere is very slight. We assume that nuclear-processed material dominates the atmosphere. We further assume that the iron-group nuclei have not been affected by processing. Synthesis of these nuclei is expected only in the cores of massive stars ending in a supernova explosion. The *s*-process will reduce the Fe-group abundances, but *s*-processing cannot have been significant in either R CrB or XX Cam. We assume that the abundances relative to iron were initially solar. This initial composition is summarized in Table 6 with the observed abundances for R CrB and XX Cam.

A stellar core is first affected by H-burning through the *p-p* chain and the CNO cycles. Prior to the onset of He burning, the CNO cycles have run to equilibrium even though the *p-p* chain may have been the dominant energy source. A low mass star will reach $T \sim 60 \times 10^6$ K in the core where the equilibrium abundances are $^{12}C/^{14}N \approx 0.03$, $^{16}O/^{14}N \approx 0.005$, and $^{12}C/^{13}C = 3.4$

TABLE 6

OBSERVED AND PREDICTED COMPOSITIONS

	Abundance Ratio log (X/Fe)						
		Stellar Core[a]					
Element	Sun	CNO	He′	He″	R CrB	XX Cam	He B Stars[b]
H.....	4.5	XXX[c]	XXX	XXX	0.2	< -2.6	0.2
He[d]	3.3	4.0	3.9	5.0	5.1 (4.2–5.2)	4.8 (4.0–5.0)	3.7
^{12}C	1.2	0.1	2.6	2.6	2.7	2.4	1.9
^{13}C	−0.7	−0.4	−0.5	−1.5	<1.1	...	...
^{14}N	0.5	1.6	1.5	1.9	1.6	1.9	1.0
^{16}O	1.4	−0.7	2.2	2.2	2.3	2.2	0.6

[a] The predicted composition is shown for the following exposures to nuclear burning: CNO = post H-exhausted core collapse with CNO cycles run to equilibrium for $T \sim 60 \times 10^6$ K. He′ = post He-core flash with the 3α process converting 20% of the He to C and O in the proportions 2 to 1. He″ = as for He′ but the H-exhausted core was originally metal poor (i.e., an old disk star) by a factor of 10 with a modest O overabundance (Clegg, Lambert, and Tomkin 1981). 2% of the He is burnt to C and O.

[b] Mean abundances for the 3 extreme He-rich B stars HD 124448, BD +10°2179 and HD 168476. Data from Hunger (1975). Where an upper limit was given, we adopt that limit as the abundance in compiling the mean.

[c] XXX denotes a very small abundance ratio X/Fe.

[d] For R CrB and XX Cam, upper and lower limits (see § III*a*) are shown in parentheses.

(Fowler, Caughlan, and Zimmerman 1975). Li is completely destroyed. The composition of the He-rich core prior to He ignition is given in Table 6 under the heading "CNO"; the key point is that it is N rich and C and O poor.

The onset of He burning in the core converts He to ^{12}C, quickly destroys ^{14}N (and ^{13}C) by the $^{14}N(\alpha,\gamma)^{18}F(e^+,\nu)^{18}O$ reactions and may produce ^{16}O and heavier elements from the ^{12}C nuclei by successive α captures. When ^{16}O production occurs, the ^{18}O will be destroyed by $^{18}O(\alpha,\gamma)^{22}Ne$ and $^{18}O(\alpha,n)^{21}Ne$ reactions. Since the burning may be inhomogeneous through the core, some ^{18}O may survive and be present in H-poor, C-rich atmospheres. The ^{16}O production depends on the core temperature and the duration of He burning. Note that the rate for the crucial $^{12}C(\alpha,\gamma)^{16}O$ reaction is uncertain. A key result of He burning is that ^{14}N is readily destroyed during this phase so that the observed high N abundance demands that the atmosphere now contain a mixture of CNO-cycle exposed and 3α-processed material. Table 6 shows predictions for two cases of partial He burning with the arbitrary stipulation that the C and O be produced in the proportions 2 to 1. The (uncertain) C/He ratio derived from the 5876 Å line would seem to imply that the initial star was moderately metal deficient. The quantitative correspondence between the He′ and He″ predictions in Table 6 and the observed abundance is not as significant as the general constraints set by our abundances. The present atmospheres contain a large amount of He previously exposed to the CNO cycles (the high N abundance and the fact that N is destroyed in He-burning set this constraint) with a small mixture of the products of He burning under conditions adequate to produce ^{16}O.

A nuclear history must also explain why *s*-processing has not occurred in R CrB and XX Cam. The *s*-processing in a He core or shell is most probably controlled by the neutron sources $^{22}Ne(\alpha,n)^{25}Mg$ and $^{13}C(\alpha,n)^{14}O$. The initial ^{22}Ne abundance is low, and an insufficient neutron flux (<1 per Fe seed nucleus) is supplied. Additional ^{22}Ne nuclei may be created from ^{14}N via ^{18}O and $^{18}O(\alpha,\gamma)^{22}Ne$. Then, the maximum supply is 30 to 60 neutrons per Fe seed nucleus; the higher figure pertains to metal-poor cores. It is interesting to note that Bond, Luck, and Newman (1979) report that an exposure of 30 neutrons per Fe seed nucleus is required to explain the *s*-process enhancements in U Aqr. Furthermore, the distribution of *s*-process abundances created by the ^{22}Ne source is consistent with the observed abundances of U Aqr (Lamb *et al.* 1977). Consumption of ^{22}Ne is preventable by limiting the core temperature; if $T \lesssim 2\times10^8$ K, ^{16}O production seems possible without significant neutron release from ^{22}Ne [note that at low temperatures $^{22}Ne(\alpha,\gamma)^{26}Mg$ is favored over $^{22}Ne(\alpha,n)^{25}Mg$].

The residual abundance of ^{13}C in the He burning core or shell is too low to cause significant *s*-processing by neutrons released through the $^{13}C(\alpha,n)^{16}O$ reaction at He burning. The neutron supply may be enhanced by mixing in a little H-rich material so that ^{13}C is regenerated and neutrons created from fresh ^{12}C by the chain $^{12}C(p,e^+)^{13}C(\alpha,n)^{16}O$. Such mixing will not produce an inadmissible reduction of the $^{12}C/^{13}C$ ratio as long as a small number of protons are added. This latter proviso is physically plausible because the large energy release, which must accompany the addition of protons, can be suspected of quenching any mixing process. As empirical evidence, we cite the Ba II stars where $^{13}C(\alpha,n)^{16}O$ is probably the neutron source (Tomkin and Lambert 1979) and the $^{12}C/^{13}C$ ratio is generally large (say $^{12}C/^{13}C \gtrsim 30$). For R CrB and XX Cam, we suggest that protons were not mixed into the He-burning region and, hence, *s*-processing did not occur.

In normal evolution, Li is completely destroyed in a stellar core. Even in the H-rich convective outer envelope of a normal giant, the Li abundance is a factor of 10^3 to 10^4 smaller than the abundance reported here for R CrB. The ^{7}Be transport mechanism is probably responsible for Li production in R CrB; the process involves the reactions $^3He(\alpha,\gamma)^7Be(e^-,\nu)^7Li$ where ^{3}He is produced at an earlier time from H in the initial steps of the *p-p* chain. The ^{3}He seed nuclei are probably a product of the main sequence phase (Iben 1967*a*, *b*). In a low-mass giant, where the outer envelope is predicted to contain a ^{3}He mass fraction of up to 10^{-3}, the conversion to ^{7}Li via ^{7}Be may operate at very low efficiency and yet produce the Li seen in R CrB. Since the ^{7}Be (and ^{7}Li) must be swept quickly from a hot zone to cool ($T \lesssim 10^6$ K) layers in order to survive destruction by (p,α) or (α,γ) reactions, a low efficiency is not surprising.

Spallation reactions on the stellar surface are a competing explanation for the Li in R CrB. Canal, Isern, and Sanahuja (1977) discuss production of Li by spallation. Hunger, Schönberner, and Steenbock (1982) identify spallation reactions as a possible source for Li. If spallation occurs, the $^7Li/^6Li$ ratio could be as low as 4. Our spectra of R CrB imply a Li I wavelength of 6707.82 Å relative to the Al I line at 6696.03 Å. The predicted wavelengths for pure ^{7}Li and pure ^{6}Li lines are 6707.83 Å and 6708.05 Å, respectively. (This assumes wavelengths of 6707.76 Å and 6707.98 Å for the individual lines of the ^{7}Li I doublet.) Consequently, we can rule out a pure ^{6}Li line. For $^7Li/^6Li = 4$, the shift is ~ 0.05 Å from the pure ^{7}Li line. (This corresponds to two diodes on the Reticon echelle spectrum we obtained of this region.) Combining this information with our observations, $^7Li/^6Li > 7$. Therefore, on the basis of our observations, a large contribution of lithium from spallation would be ruled out.

b) *R Coronae Borealis Variables and Stellar Evolution*

Our sketch of the nuclear history of the R CrB atmosphere must be integrated into a full evolutionary history for these unusual stars. The internal structure in the R CrB phase probably consists of a thin He-rich envelope around a carbon-oxygen core. Schönberner (1977) traced the evolution of such low mass (0.65–1 $\mathfrak{M}_\odot$ stars. Within about 10^4 yr, the R CrB star has evolved to a He-rich B star and on to become a white dwarf. Recently, Heber and Schönberner (1981) have claimed that the observed galactic density of R CrB and He B stars is consistent with evolution from supergiant (R CrB) to dwarf (He B star) as modeled by Schönberner (1977). Kilkenny (1982) analyzed photometric observations of RY Sgr spanning a 50 year period to show that the pulsational period is decreasing at a rate consistent with Schönberner's models.

This proposed evolutionary coupling of R CrB and He-rich B stars is perhaps challenged by the results on the chemical composition. Hunger (1975) has assembled the data for the He-rich stars (see Table 6). Striking differences in composition between the R CrB and He-rich B stars may be noted: the latter are C, N, and O poor relative to the R CrB stars when the abundance ratios X/Fe are compared. If He-rich B stars are evolved R CrB stars, a closer similarity of composition is expected. It should be emphasized that abundance data are currently available in detail for just two R CrB stars and very few of the B stars. The possibility exists that the chemical compositions of both classes span a broad range and that similarities will emerge only when larger samples have been analyzed.[3]

The evolutionary history must also account for the origin of R CrB stars. On the assumption that ejection of the H-rich outer envelope is a prerequisite for R CrB formation, the asymptotic giant branch (AGB) is an attractive location for the first appearance of He-rich stars. Envelope instabilities affecting AGB stars are possibly responsible for mass ejection leading to the formation of planetary nebulae. Härm and Schwarzschild (1975) showed that such instabilities could leave the star with a very thin H envelope. Continued mass loss either as a steady wind or in bursts would produce a He-rich star. Thus one could envisage a connection between the R CrB stars and the He- and C-rich ejecta of two planetary nebulae, Abell 30 and 78 (Jacoby and Ford 1982).

Ejection of the H-rich envelope through explosion may also occur at the He core flash, as a low-mass ($< 2.5\ \mathfrak{M}_\odot$) star reaches the tip of the first red giant branch. Deupree and Cole (1981) in a hydrodynamical analysis of the He-core flash show that, although a prediction of the nucleosynthesis is beset with considerable uncertainties, a substantial amount of ^{4}He is processed to ^{12}C, and a fraction is further processed to ^{16}O. They predict that significant mass loss could occur at the He core flash. With this ejection and some mixing of the 3α processed material with the outer portions of the He-rich envelope, a star with abundances resembling those which we have derived for the R CrB stars could result. The high luminosities exhibited by these stars could be attained by requiring the stars to have a Si core (Dearborn, private communication), while burning He in a shell.

An alternative hypothesis which combines elements of both those which we have discussed above could also be considered as a site for both the He-rich B stars and the R CrB variables. It is possible that some of the abundance differences which are observed between these two groups of stars are determined by the violence of the core flash and the extent of nuclear processing within the core. Indeed, these may be the parameters which determine whether a star proceeds with a normal evolution or becomes a more bizarre object—e.g., an R CrB or CH star. The small number of these objects certainly implies that the process occurs quite infrequently. In addition, a short lifetime for the R CrB stars is also ensured since the He-shell flash stage is relatively short compared with the He-core burning phase. This in turn leads to a paucity of these objects.

VII. CONCLUDING REMARKS

Our abundance analysis of R CrB and XX Cam, which has provided new data on key light elements C, N, and O, is consistent with the identification of the present atmospheres as portions of an exhausted H-burning core or shell into which has been mixed a small amount of material from a He burning core or shell. This mixture accounts for the relative abundance of most elements. In particular, N is provided solely by the exhausted H-burning regions, and C and O by the He burning zones.

With the advent of linear detectors of high quantum efficiency in spectrographs on large telescopes, the opportunity is now available to extend the abundance analyses to a larger sample of R CrB and other H-deficient peculiar stars—e.g., the CH stars, the W Vir Cepheid-like variables (see Luck 1981 for the suggestion that these may be H-poor), the HdC carbon stars, and the He-rich B stars.

As our discussion of the nuclear history demonstrates, these analyses should be comprehensive; and, in particular, Li, C, N, O and the *s*-process elements should be included. A measurement of ^{6}Li/^{7}Li ratio in a sharp-lined R CrB star would test the spallation hypothesis more fully. If the CO vibration-rotation bands can be detected in the photospheric or circumstellar spectra, a

[3]Recent work by Heber (Schönberner, private communication) indicates that some similarities are emerging.

search for ^{18}O, from ^{14}N destruction, should be undertaken.

We thank Dr. D. Schönberner for sending us a copy of his model atmosphere grid, in addition to his many constructive comments on the original manuscript, Dr. J. Tomkin for assistance at the telescope, and Drs. D. S. P. Dearborn, J. C. Wheeler and J. M. Scalo for helpful discussions. In addition, we should like to thank J. F. Dominy, S. W. Roby, and Dr. R. E. Luck for their help with data reduction and analysis techniques. This research was supported in part by grants from the National Science Foundation (AST 79-22014 and 81-17485) and the Robert A. Welch Foundation of Houston, Texas.

REFERENCES

Alexander, J. B., Andrews, P. J., Catchpole, R. M., Feast, M. W., Lloyd Evans, T., Menzies, J. W., Wisse, P. N. J., and Wisse, M. 1972, *M.N.R.A.S.*, **158**, 305.
Bidelman, W. P. 1953, *Ap. J.*, **117**, 25.
Bond, H. E., Luck, R. E., and Newman, M. J. 1979, *Ap. J.*, **233**, 205.
Canal, R., Isern, J., and Sanahuja, B. 1977, *Ap. J.*, **214**, 189.
Clegg, R. E. S., Lambert, D. L., and Tomkin, J. 1981, *Ap. J.*, **250**, 262.
Cox, J. P., King, D. S., Cox, A. N., Wheeler, J. C., Hansen, C. J., and Hodson, S. W. 1980, *Space Sci. Rev.*, **271**, 529.
Danziger, I. J. 1965, *M.N.R.A.S.*, **130**, 199.
Delbouille, L., Roland, G., and Neven, L. 1973, *Photometric Atlas of the Solar Spectrum from λ3000 to λ10000* (Liège: Institut d'Astrophysique).
Deupree, R. G., and Cole, P. W. 1981, *Ap. J. (Letters)*, **249**, L35.
Feast, M. W. 1975, in *IAU Symposium 67, Variable Stars and Stellar Evolution*, ed. V. E. Sherwood and L. Plaut (Dordrecht: Reidel), p. 129.
Fernie, J. D. 1982, *Pub. A.S.P.*, **94**, 172.
Fowler, W. A., Caughlan, G. R., and Zimmerman, B. A. 1975, *Ann. Rev. Astr. Ap.*, **13**, 69.
Härm, R., and Schwarzschild, M. 1975, *Ap. J.*, **200**, 234.
Heber, U., and Schönberner, D. 1981, *Astr. Ap.*, **102**, 73.
Holweger, H., and Müller, E. A. 1974, *Solar Phys.*, **39**, 19.
Hunger, K. 1975, in *Problems in Stellar Atmospheres and Envelopes*, ed. B. Baschek, W. H. Kegel, and G. Traving (New York: Springer-Verlag), p. 57.
Hunger, K., Schönberner, D., and Steenbock, W. 1982, *Astr. Ap.*, **107**, 93.
Iben, I., Jr. 1967*a*, *Ap. J.*, **147**, 624.
_____. 1967*b*, *Ap. J.*, **147**, 650.
Jacoby, G. H., and Ford, H. C. 1982, *Bull. AAS*, **13**, 854.
Keenan, P. C., and Greenstein, J. L. 1963, *Contr. Perkins Obs.*, **2**, 13.
Kilkenny, D. 1982, preprint.
Kurucz, R. L. 1970, *SAO Spec. Rept.*, No. 309.
Kurucz, R. L., and Peytremann, E. 1975, *SAO Spec. Rept.*, No. 362.
Lamb, S. A., Howard, W. M., Truran, J. W., and Iben, I., Jr. 1977, *Ap. J.*, **217**, 213.
Lambert, D. L. 1968, *M.N.R.A.S.*, **138**, 143.
_____. 1978, *M.N.R.A.S.*, **182**, 249.
Luck, R. E. 1981, *Pub. A.S.P.*, **93**, 211.
_____. 1982, preprint.
Luck, R. E., and Lambert, D. L. 1981, *Ap. J.*, **245**, 1018.
Myerscough, V. P. 1968, *Ap. J.*, **153**, 421.
Myerscough, V. P., and McDowell, M. R. C. 1966, *M.N.R.A.S.*, **132**, 457.
Orlov, M. Ya., and Rodriguez, M. H. 1974, *Astr. Ap.*, **31**, 203.
Peach, G. 1970, *Mem. R.A.S.*, **73**, 1.
Querci, M., and Querci, F. 1978, *Astr. Ap.*, **70**, L45.
Rao, N. K., Ashok, N. M., and Kulkarni, P. V. 1980, *J. Ap. Astr.*, **1**, 71.
Richter, J. 1961, *Zs. Ap.*, **51**, 177.
Ross, J. E., and Aller, L. H. 1976, *Science*, **191**, 1223.
Schönberner, D. 1975, *Astr. Ap.*, **44**, 383.
_____. 1977, *Astr. Ap.*, **57**, 437.
Searle, L. 1961, *Ap. J.*, **133**, 531.
Sneden, C. 1974, unpublished Ph.D. thesis, University of Texas.
Tomkin, J., and Lambert, D. L. 1979, *Ap. J.*, **227**, 209.
Travis, L. D., and Matsushima, S. 1968, *Ap. J.*, **154**, 689.
Vogt, S. S., Tull, R. G., and Kelton, P. K. 1978, *Appl. Optics*, **17**, 574.
Wiese, W. L., Smith, M. W., and Glennon, B. M. 1966, *Atomic Transition Probabilities*, Vol. **1** (NSRDS–NBS4).
Zirin, H. 1982, *Ap. J.*, **260**, 655.

P. L. COTTRELL: Department of Physics, University of Canterbury, Christchurch 1, New Zealand

D. L. LAMBERT: Department of Astronomy, University of Texas, Austin, TX 78712